Int. J. Rock Mech. & Min. Sci. Vol. 34, No. 3-4, 1997
ISSN 0148-9062

To cite this paper:
Int. J. Rock Mech. & Min. Sci. **34:3-4**, Paper No. 232

MODELING OF DEFORMATION AND POROSITY CHANGE FROM NORMAL FAULTING[1]

Rui Chen, John A. Stamatakos, David A. Ferrill, and Goodluck I. Ofoegbu

Center for Nuclear Waste Regulatory Analyses
6220 Culebra Road
San Antonio, TX 78238-5166, USA

ABSTRACT

The near-surface tectonic setting at Yucca Mountain (YM), the proposed site for permanent storage of high-level radioactive nuclear waste, is characterized by a system of extensional faults in a highly jointed rock mass. Rupture along active fault zones in a jointed rock mass may cause changes in joint aperture, which could alter hydraulic conductivity of the rock mass. In particular, it has been suggested that normal faulting could cause significant dilation of the rock mass, thereby, increase fluid flow in hangingwalls and within fault zones. As a result, the effects of normal faulting on rock-mass permeability are being investigated to assess possible impacts on groundwater flow and infiltration. The purpose of the current study is to investigate this process and briefly discuss its significance to effective and safe isolation of high-level nuclear waste at YM.

Fully coupled mechanical-hydraulic analyses were conducted using the distinct element code UDEC to examine changes in joint aperture due to normal faulting. It was assumed in the analyses that fluid pressure was hydrostatic and joint blocks were impermeable and bounded by permeable joints (i.e., flow through joints only). Fault layout of the distinct element model was constructed based on an east-west vertical cross section through the proposed repository at YM. Model configuration consists of three fault zones and two hypothetical regional scale joint sets (vertical and horizontal) above a basal substructure that was assumed to be unjointed for the purposes of model simplification. The fault zones were constructed to simulate three major fault zones near the proposed repository, namely the Solitario Canyon, Ghost Dance, and Bow Ridge faults. Simulation started with an initial static analysis to achieve steady-state, *in situ* mechanical and hydraulic conditions, followed by 1 m displacement of the three fault zones in pre-defined sequences. Displacement of each fault zone was simulated by applying shear displacement directly to the entire fault zone. After each fault slip, model response was monitored until a new equilibrium was reached to allow full recovery of stresses and deformation. Joint aperture changes due to each faulting event were examined and corresponding changes in the average rock mass porosity were estimated.

Modeling results show that fault slip creates a disturbed zone along the activated fault within which joint dilation (increase in joint aperture) occurs. The extent of the disturbed zone and the direction of joint

[1]Work supported by the U.S. Nuclear Regulatory Commission (NRC, Contract NRC-02-93-005). This research is an independent product of the Center for Nuclear Waste Regulatory Analyses and does not necessarily reflect the views or the regulatory position of the NRC.

dilation are controlled by the dip angle of the activated fault. Slip on higher angle faults results in a narrower disturbed zone and greater dilation of vertical (subvertical) joints. Slip on lower angle faults produces a wider disturbed zone and greater dilation of horizontal (subhorizontal) joints. Estimation of porosity changes due to fault slip shows that the average rock mass porosity could increase by two orders of magnitude in terms of percentage changes due to a 1 meter rupture along an individual fault zone. At least 95 percent of the increased porosity occurs in the disturbed zone along the ruptured fault. Such significant increase in rock mass porosity would generally increase rock mass permeability and fluid flow. Formation of the disturbed zone along the activated fault may also create fast pathways for infiltration of water from surfaces. Secondary slip along faults close to or within the proposed repository area could be triggered by slip along another regional fault, which may induce mechanical effects on waste package integrity and drift stability.

KEYWORDS

Normal faulting, jointed rock, joint aperture, deformation, fluid flow, radioactive waste

Int. J. Rock Mech. & Min. Sci. Vol. 34, No. 3-4, 1997
ISSN 0148-9062

To cite this paper:
Int. J. Rock Mech. & Min. Sci. **34:3-4**, Paper No. 232

3/13

MODELING OF DEFORMATION AND POROSITY CHANGE FROM NORMAL FAULTING

Rui Chen, John A. Stamatakos, David A. Ferrill, and Goodluck I. Ofoegbu

Center for Nuclear Waste Regulatory Analyses
6220 Culebra Road
San Antonio, TX 78238-5166, USA

ABSTRACT

Rupture along active fault zones in a jointed rock mass may cause changes in joint aperture, resulting in changes in hydraulic conductivity of the rock mass. Normal faulting, in particular, could cause significant joint dilation and increase fluid flow near fault zones. This paper investigates joint dilation from normal faulting and briefly discusses its significance to the effective and safe isolation of high-level nuclear waste at the proposed Yucca Mountain (YM) repository. Fully coupled mechanical-hydraulic analyses were conducted on a model constructed based on an east-west vertical cross section through the proposed repository at YM. Fault slip was simulated by applying shear displacement directly to the fault zone. Modeling results show that slip along the entire fault creates a disturbed zone along the activated fault. Within the disturbed zone, significant joint dilation (increase in joint aperture) occurs. The extent of the disturbed zone and the direction of joint dilation are strongly controlled by the dip angle of the activated fault. Slip on higher angle faults induces a narrower disturbed zone and greater dilation of vertical (subvertical) joints. Slip on lower angle faults produces a wider disturbed zone and greater dilation of horizontal (subhorizontal) joints. Estimation of porosity changes due to fault slip shows that the average rock mass porosity could increase by two orders of magnitude in terms of percentage changes due to a 1 m fault rupture. Joint dilation and increase in porosity from normal faulting not only increase rock mass permeability and the possibility of groundwater flow near the repository, but may also create faster pathways for infiltration of surface water.

KEYWORDS

Normal faulting, numerical analysis, jointed rock, joint aperture, deformation, fluid flow, radioactive waste

INTRODUCTION

Fault related deformation in fault blocks and fault zones can cause significant changes in joint aperture, thereby altering porosity, permeability, and hydraulic conductivity of the rock mass. Zhang and Sanderson (1996) studied deformation in regions of jointed rock around an extensional fault using a simple model of a planar normal fault zone. They observed significant dilation and fluid flow in the

hangingwall and within the fault zone itself during faulting. Although there are a number of technical problems associated with the modeling approaches and boundary conditions in Zhang and Sanderson's simulation (Chen and Lorig, 1997), their observations have practical significance. Most importantly, their attempt indicates that when applied appropriately, numerical experiments based on a discontinuum mechanics approach can be used to explore the mechanisms controlling faulting related joint dilation and fluid flow. Similar mechanisms may also control many other fluid-flow related phenomena accompanying faulting observed *in situ*, like episodic fluid flow near active faults (Sibson, 1988, 1990 and 1994; Logon, 1994), fault controlled fluid migration and mineralization (Munroe 1995), and pore pressure changes accompanying normal faulting (Rudnicki, 1991). Faulting also affects fluid flow in other porous rock masses, such as sandstones (Antoellini and Aydin, 1995). The fact that most of these phenomena have been associated with normal faulting indicates the importance of normal faulting in controlling rock mass hydraulic properties and fluid flow.

Changes in rock mass hydraulic properties and fluid flow associated with normal faulting are particularly important at Yucca Mountain (YM), the proposed site for permanent disposal of high-level radioactive nuclear waste, because the near surface tectonic setting at YM is characterized by a system of extensional faults (Scott, 1990; Young et al. 1992) and highly jointed fault blocks (Brechtel and Kessel, 1995; Brechtel, et al., 1995). Such faulting induced changes in joint aperture imply that normal faulting at YM, in the future, may increase rock mass permeability within the perturbed region, especially along the activated as well as existing fault zones. It may facilitate flow of groundwater in the saturated zone below the repository and provide a faster path for infiltration in the unsaturated zone above the repository, and thereby, affect the effective and safe isolation of high-level nuclear waste. As a defensive measure, the Department of Energy (DOE) is considering an offset distance from the faults for emplacement of waste.

In the present study, fully coupled mechanical-hydraulic analyses were conducted of a normal fault model analogous to the YM fault system. The distinct element code UDEC (Itasca Consulting Group, Inc., 1996) was used to examine changes in joint aperture from normal faulting. Subsequent changes in the average rock mass porosity were then estimated for each fault block, for all fault blocks combined, and for the entire model. The significance of these modeling results are discussed in regard to effective and safe isolation of high-level nuclear waste at YM.

MODEL DESCRIPTION

The distinct element model was constructed based on an east-west vertical cross section through the proposed repository at YM taken from the Center for Nuclear Waste Regulatory Analyses (CNWRA) three-dimensional geological framework model for YM (Stirewalt and Henderson, 1995). The model configuration for the distinct element analyses consists of three fault zones labeled as Faults 1 through 3 in Figure 1. These fault zones are analogous to the three major fault zones near the proposed repository, namely the Solitario Canyon, Ghost Dance, and Bow Ridge Faults. Each fault is represented by a 75 m wide zone which is assumed to be highly fractured with two orthogonal joint sets parallel and perpendicular to the fault zone. The joint spacing for both joint sets within the fault zones is 25 m. Fault blocks are labeled as Blocks 1 through 4. Each fault block contains two hypothetical regional scale joint sets, horizontal and vertical, respectively. Joint spacing is 100 m for the vertical joint set and 200 m for the horizontal joint set, reflecting observations at YM that spacing of vertical (subvertical) joints is much smaller than that of horizontal joints (Brechtel and Kessel 1995; Brechtel et al., 1995). All of the fault zones and fault blocks were assumed to be above a basal substructure that is assumed to be unjointed for purposes of model simplification.

The top boundary of the model was assumed to be a stress-free boundary, simulating the ground surface. Other boundaries were modeled as boundary-element boundaries. A boundary-element boundary is an artificial boundary that simulates the semi-infinite extent of isotropic, linear, elastic material (Itasca

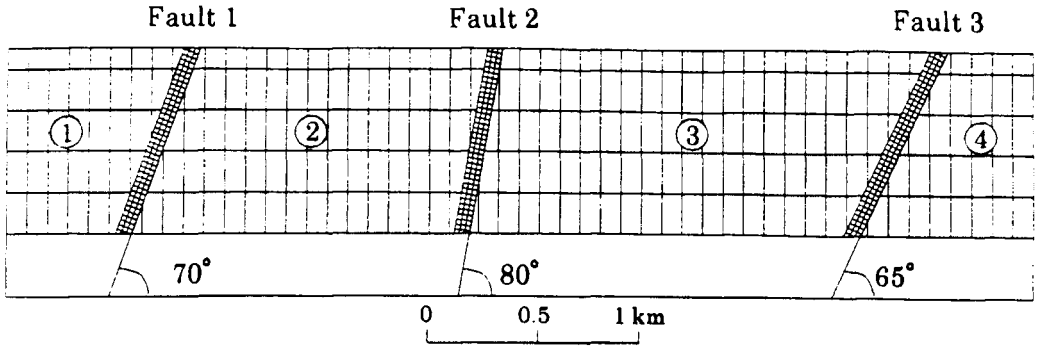

Figure 1: Geometry of YM fault model. Fault zones are modeled as 75 m wide zones with two orthogonal joint sets. There are two regional joint sets (vertical and horizontal) with spacings of 100 m and 200 m, respectively.

Consulting Group, Inc., 1996). Boundary element boundaries are, therefore, a realistic simulation of the subsurface conditions. The fluid pressure in the model was assumed to be hydrostatic, i.e., 9.81 MPa/km, and the model was assumed to be saturated with water. The hydraulic boundaries were pressure boundaries selected such that the fluid pressure in the entire model remains hydrostatic. The hydraulic pressure along the top and bottom boundaries was 0 and 11.772 MPa (at 1200 m depth), respectively. Hydraulic pressure along left and right boundaries increases linearly downward. The *in situ* stresses are the total stresses that include vertical stress caused by gravity, horizontal stress related to vertical stress by an assumed Poisson's ratio given in Table 1, and hydrostatic fluid pressure caused by the weight of pore water. For modeling, it was assumed that intact rock blocks were impermeable and bounded by permeable joints.

Intact rock blocks were modeled as a linear elastic material. Rock joints were modeled according to Mohr-Columbous failure criterion. Mechanical and hydrologic properties were selected to represent the host rock of the proposed repository at YM, the Topopah Spring welded tuff, based on a number of sources as summarized in Ahola et al. (1996). Those properties are also given in Table 1. Figure 2 shows the uniform distribution of joint aperture before fault slip.

MODELING APPROACH

Modeling initiated with a static analysis to achieve steady-state, *in situ* mechanical and hydraulic conditions. The initial analysis was followed by 1 m displacement of the three fault zones in pre-defined sequences. Fault slip was simulated by applying shear displacement directly to the entire fault zone, which was achieved by applying a velocity parallel to the fault zone to grid points along the fault zone and using the FISH functions available in UDEC vision 3.00 (Itasca Consulting Group, Inc., 1996) to fix velocity over a certain length of time (0.5 s in this case) that would accumulate the desired total shear displacement (1 m in this case) along the fault zone in a stable fashion. The direction of the velocity applied to grid points was upward parallel to the fault zone in the hangingwall, and downward parallel to the fault zone at grid points in the footwall. After each fault slip, the model response was monitored

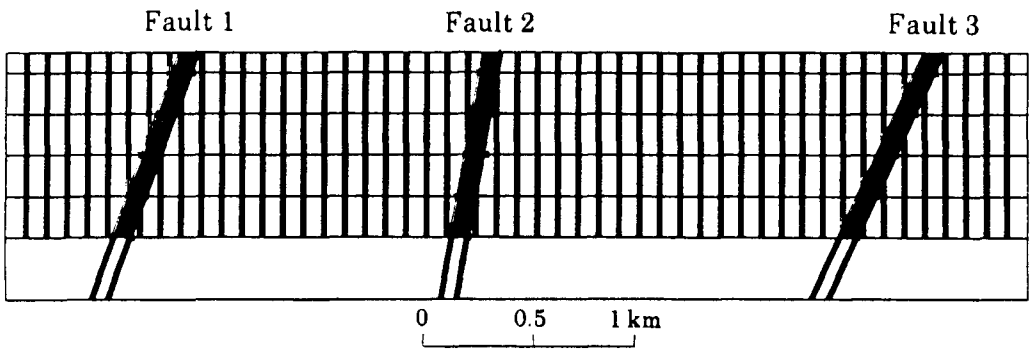

Figure 2: Uniform distribution of joint aperture before fault slip. The initial joint aperture is 0.001 m for vertical joints and 0.0005 m for horizontal joints.

until a new equilibrium was reached before simulating the next fault slip to allow full recovery of stresses and deformation. Joint aperture changes due to each fault slip were then examined and corresponding changes in porosity were estimated.

In UDEC, a rock joint is represented numerically as a contact surface formed between two block edges. A contact surface between two deformable blocks is composed of individual point contacts, each with a definite contact length to form a domain. Joint hydraulic aperture, a, at a specific contact is given, in general, by:

$$a = a_0 + u_n \tag{1}$$

where a_0 is joint aperture at zero normal effective stress, and u_n is the joint normal displacement. For the current study, a residual aperture is assumed below which mechanical closure does not affect the contact permeability (see Table 1). The upper bound of the hydraulic aperture is identical to the mechanical aperture.

The average percentage porosity, ϕ, in a specific area of interest, S, was approximately estimated as:

$$\phi = \frac{\sum_{i=1}^{n} (a_i \times l_i)}{S} \times 100\% \tag{2}$$

where a_i and l_i are hydraulic aperture and domain length at contact i, n is the total number of contacts at the time ϕ is estimated within a specific area S.

TABLE 1
MATERIAL MECHANICAL AND HYDRAULIC PROPERTIES

Parameters		Units	Values
Intact Block Parameters			
Young's Modulus		GPa	32.3
Poisson's Ratio		-	0.21
Density		kg/m^3	$2.297(10^3)$
Rock Joint Parameters			
Normal Stiffness		GPa	13.46
Shear Stiffness		GPa	24.3
Cohesion		MPa	0.08
Friction Angle		°	35
Tensile Strength		MPa	0.04
Dilation Angle		°	5
Residual Aperture	Vertical Joints	m	0.0002
	Horizontal Joints	m	0.0001
Zero Stress Aperture	Vertical Joints	m	0.001
	Horizontal Joints	m	0.0005
Fluid Parameters			
Density		kg/m^3	1000
Bulk Stiffness		MPa	$3.0\ (10^3)$

DESCRIPTION OF MODELING RESULTS

The two most significant modeling results that directly affect hydraulic conductivity of the rock mass are joint dilation and subsequent changes in joint permeability. Other factors, such as joint connectivity, joint shear displacement, and changes in stress state near the activated fault zones, may also affect rock mass hydraulic properties. However, evaluation of these effects is rather complicated and involves sophisticated estimation of a permeability tensor for a jointed rock mass (Zhang et al., 1996), which is beyond the scope of the current paper.

Joint Aperture

The most significant disturbance to a jointed rock mass from normal faulting is joint dilation, reflected by changes in joint aperture. Figures 3a through 3c show the distribution of joint aperture after each fault slip in the sequence of 3-2-1. In these figures, the thickness of the solid lines is proportional to the magnitude of the joint aperture. Joint apertures greater than 0.01 m or less than 0.002 m are not included

for clarity. These figures show that slip on each fault zone creates a disturbed zone along the activated fault. Joint aperture increases along both horizontal and vertical joints within the disturbed zone. The width of the disturbed zone appears to be controlled by the dip angle of the activated fault. Higher angle fault (Fault 2) generates narrower disturbed zones, while lower angle fault (Fault 1) generates wider disturbed zones. The dip angle of the activated fault also appears to control the orientation of joint dilation. Greater dilation occurs along vertical joints following slip along higher angle faults, while greater dilation occurs along horizontal joints following slip along lower angle faults.

In general, dilation along vertical joints occurs in the immediate neighborhood of the activated fault, while dilation along horizontal joints extends to a considerable distance ($\approx$600 m) away from the activated fault zone. This joint structural characteristic within the disturbed zone greatly increases the potential for fluid flow along the fault zone. Particularly, dilation along horizontal-subhorizontal joints creates pathways that could lead water bodies perched in the fault blocks to flow to the opened vertical joints and the fault zone, and to drain downward along these channels. In Block 2, the disturbed zones from combined slip events along Faults 1 and 2 are almost interconnected.

Another phenomenon that may have significance to the performance of the proposed YM repository is that slip on Fault 3 induces both normal and shear displacements along Faults 1 and 2. These secondary normal displacements are demonstrated by increased aperture along Faults 1 and 2 after slip on Fault 3 (Figure 3a). Similar secondary shear displacement can be observed from plots of joint shear displacement after each fault slip event. Fault 2 represents the Ghost Dance fault that extends through the proposed repository area. These results suggest that a slip event on another fault zone in YM region could trigger secondary slip on the Ghost Dance fault. Secondary rupture on faults within the repository block is an important consideration for performance analyses of the mechanical effects on waste package integrity and drift stability due to faulting and seismicity.

Rock Mass Porosity

Initial porosity and porosity after each fault slip event were calculated for each of the four fault blocks, for all fault blocks combined, and for the entire model. Porosity change within the activated fault could not be correctly simulated because displacement along the fault is prescribed. Figure 4 compares the initial average rock mass porosity with porosity after a single fault slip event on each of the three faults. The comparison is made for porosity in Block 2, Block 3, the average porosity of all of the fault blocks, and the average porosity of the entire model. Blocks 2 and 3 are of particular interest because they correspond to regions within the proposed repository at YM. The numbers above the columns indicate percentage changes in the average porosity with respect to the initial porosity. Slip on Fault 1 caused about 174 percent increase of porosity in Block 2, 137 percent increase in the average porosity in all blocks, and 114 percent increase in the average porosity of the entire model. Slip on Fault 1 had very little effect in Block 3. Slip on Fault 2 caused similar porosity changes (about 190 percent) in Blocks 2 and 3, 123 percent increase in the average porosity of all fault blocks, and about 70 percent increase in the entire model. Slip on Fault 3 had little effect on Block 2. It caused 272 percent porosity increase in Block 3, 150 percent increase in the average porosity of all fault blocks, and about 130 percent increase in the entire model. As Figure 3 shows, over 95 percent of changes in porosity associated with each fault slip event occur within the disturbed zone along the activated fault.

Table 2 compares percentage changes in rock mass average porosity due to the combined effect of slip events on all three faults in different sequences. In general, the slip sequence does not significantly affect total changes in porosity. However, porosity change in Block 3 is much less when the fault slip sequence is 3-2-1. It appears that some of the joints that opened up during slip on Fault 3 were closed after slip on Fault 2.

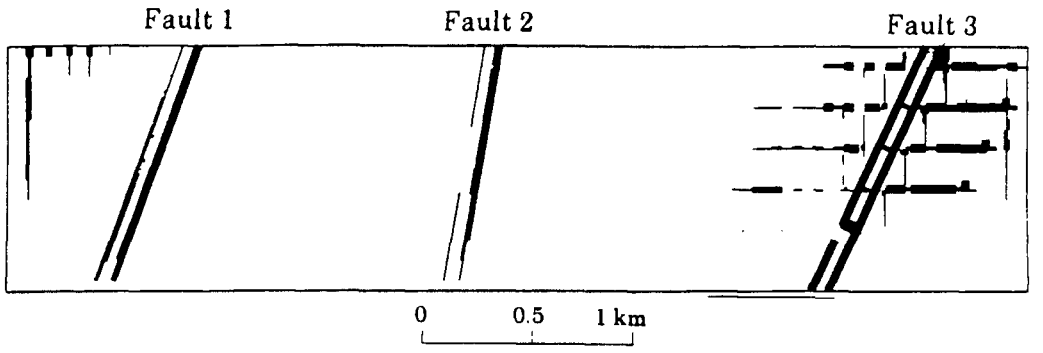

(a) After slip on Fault 3 only

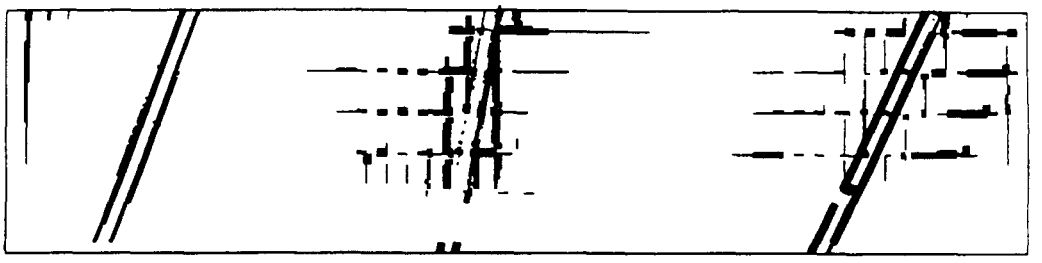

(b) Slip on Fault 2 after slip on Fault 3

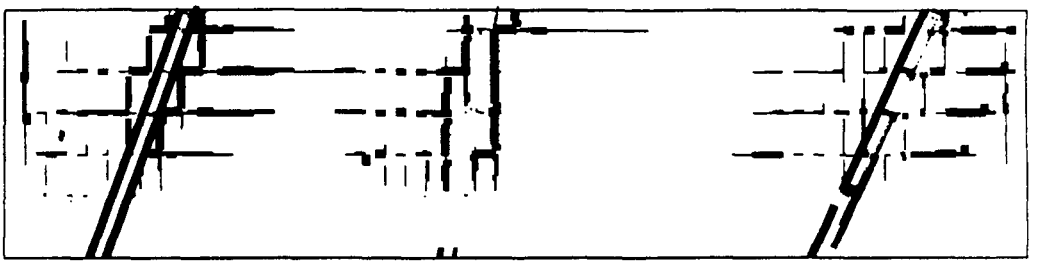

(c) Slip on Fault 1 after slip on Faults 2 and 3

Figure 3: Distribution of joint aperture after fault slip. Each line represents 0.002 m aperture. The thickest part of the line group has five lines. Apertures greater than 0.01 m and less than 0.002 m are not included for clarity. The white area, therefore, has joint aperture less than 0.002 m.

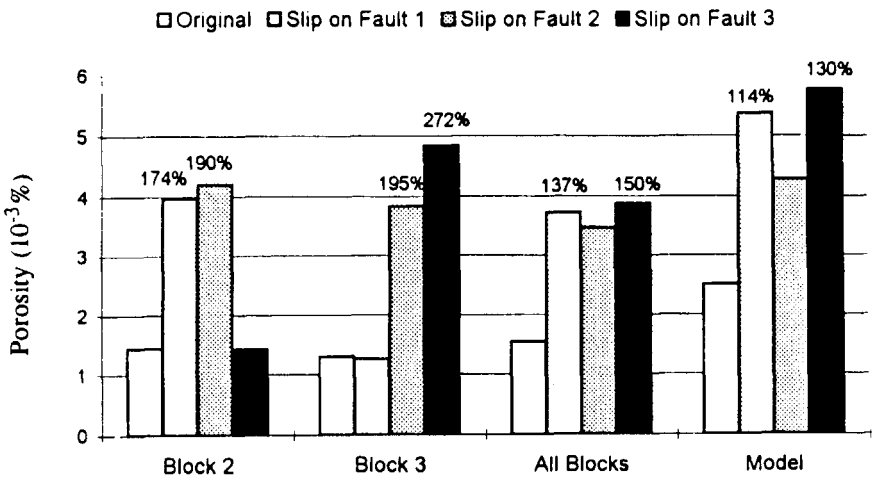

Figure 4: Comparison of the initial average rock mass porosity with porosity after a single fault slip

TABLE 2
POROSITY CHANGES (PERCENTAGE INCREASE) DUE TO COMBINED EFFECTS OF FAULT SLIP ALONG ALL THREE FAULTS IN DIFFERENT SEQUENCES

Slip Sequence	Block 2	Block 3	All Blocks	Entire Model
1-2-3	250	587	367	261
2-1-3	293	594	396	287
3-2-1	257	360	337	213

CONCLUSIONS AND DISCUSSIONS

Current modeling results show that fault slip can increase joint aperture and rock mass porosity. Rupture along the entire fault zone creates a disturbed zone along the activated fault zone and significant joint dilation occurs in the disturbed zone. Both the distribution and direction of joint dilation are strongly influenced by the dip angle of the ruptured fault. Rupture along higher angle faults produces narrower disturbed zones and greater dilation along vertical (subvertical) joints; rupture along lower angle faults produces wider disturbed zones and greater dilation along horizontal (subhorizontal) joints.

Fault slip appears to increase the average rock mass porosity by two orders of magnitude in terms of percentage change due to a 1 meter rupture along an individual fault zone. At least 95 percent of these increases in porosity occur in the disturbed zone along the ruptured fault. Such significant increases in rock mass porosity would certainly affect permeability and, hence, flow of ground water. The disturbed zone along the activated fault could create preferential faster pathways for infiltration of surface water. In addition, slip events could trigger secondary faulting thereby affecting the mechanical integrity of waste package and drift stability.

Changes in porosity associated with each fault slip analyzed in the current study do not reflect porosity changes that may occur in geologic time between successive fault slip events. The calculations only address the potential for change immediately following an earthquake produced by normal faulting. Other processes that could reduce porosity over time, such as fracture filling and other geochemical processes or the compressive effects of *in situ* stress, are not considered.

ACKNOWLEDGMENTS

The work was supported by the United States Nuclear Regulatory Commission (NRC) under contract number NRC-02-93-005, on behalf of the NRC Office of Nuclear Material Safety and Safeguards, Division of Waste Management. The views expressed in the paper are those of the authors and do not necessarily reflect the views or regulatory position of the NRC. The authors are grateful to L. Lorig of ITASCA Consulting Group, Inc for his assistance in UDEC application. We would also like to thank Drs. L. McKague and B. Sagar for their technical and programmatic reviews and their insightful comments which were of assistance in preparing the final manuscript.

REFERENCES

Ahola et al. (1996). *A Parametric Study of Drift Stability in Jointed Rock Mass, Phase I: Discrete Element Thermal-Mechanical Analysis of Unbackfilled Drifts. CNWRA 96-009.* San Antonio, TX: Center for Nuclear Waste Regulatory Analyses.

Antoellini, M. and A. Aydin. (1995). Effect of faulting on fluid flow in porous sandstones; geometry and spatial distribution. *AAPG Bulletin* **79**, 642-671.

Brechtel, C.E. and D.S. Kessel. (1995). *Geotechnical Characterization of the North Ramp of the Exploratory Studies Facility: Volume I - Data Summary.* SAND95-0488/1. Albuquerque, NM: Sandia National Laboratories.

Brechtel, C.E., M. Lin, E. Martin, and D.S. Kessel. (1995). *Geotechnical Characterization of the North Ramp of the Exploratory Studies Facility: Volume II - NRG Corehole Data Appendices.* SAND95-0488/2. Albuquerque, NM: Sandia National Laboratories.

Chen R. and L. Lorig. (1997). Discussion on 'Numerical modeling of the effects of fault slip on fluid flow around extensional faults' by Zhang, X. and D.J. Sanderson. Submitted to *Journal of Structural Geology.*

Itasca Consulting Group, Inc. (1996). *UDEC Version 3.0 User's Manual.* Minneapolis, MN: Itasca Consulting Group.

Logon, J.M. and C.L. Decker. (1994). Cyclic fluid flow along faults. *Proceedings of Workshop LXIII;* USGS Red-Book conference on the Mechanical Involvement of Fluids in Faulting, Hickman, SH.; R.H. Sibson, and R.L. Bruhn (ed.). U.S. Geological Survey, Reston, VA.

Munroe, S.M. (1995). The Porgera gold deposit, Papua New Guinea; the influence of structure and tectonic setting on hydrothermal fluid flow and mineralization at a convergent plate margin. *Proceedings of the 1995 PACRIM Congress; Exploring the rim, Mauk, J.L. and J.D. St. George ed.). Publication Series - Australiasian Institute of Mining and Metallurgy* **9/96**: 413-416.

Rudnicki, J.W. (1991). Pore pressure changes and fluid flow induced by opening accompanying normal faulting earthquakes. *Eos, Transactions, American Geophysical Union* **72**: 120-121.

Scott, R.B. (1990). Tectonic setting of Yucca Mountain, southwest Nevada. Basin and Range extensional tectonics near the latitude of Las Vegas, Nevada. B.P. Wernicke, ed. *Geological Society of America Memoir* **176**: 251-282.

Sibson, R.H. (1988). Earthquake faulting, induced fluid flow, and fault-hosted gold-quartz mineralization. *Proceedings of the International Conference on Basement Tectonics* **8**: 603-641.

Sibson, R.H. (1990). Cyclic fluid flow related to fault loading in different tectonic regimes. *Abstracts - Geological Society of Australia* **31**: 65-66.

Sibson, R.H. (1994). Crustal stress, faulting and fluid Flow. *Geofluids; origin, migration and evolution of fluids in sedimentary basins,* Parnell, J. (ed.). Geological Society Special Publications, **78**: 69-84.

Stirewalt, G.L. and D.B. Henderson. (1995). *A Three-Dimensional Geological Framework Model for Yucca Mountain, Nevada, with Hydrologic Application: Report to Accompany 1995 Model Transfer to the Nuclear Regulatory Commission. CNWRA 94-023.* San Antonio, TX: Center for Nuclear Waste Regulatory Analyses.

Young, S.R., G.L. Stirewalt, and A.P. Morris. (1992). *Geometric Models of Faulting at Yucca Mountain. CNWRA 92-008.* San Antonio, TX: Center for Nuclear Waste Regulatory Analyses.

Zhang, X. and D.J. Sanderson. (1996). Numerical modelling of the effects of fault slip on fluid flow around extensional faults. *Journal of Structural Geology* **18**: 109-119.

Zhang, X., D.J. Sanderson, R.M. Harkness, and N.C. Last. (1996). Evaluation of the 2-D permeability tensor for fractured rock masses. *International Journal of Rock Mechanics, Mining Sciences & Geomechanics Abstracts* **33**: 17-37.

232

Modeling of Deformation and Porosity Change from Normal Faulting

Chen
Rui
Center for Nuclear Waste Regulatory Analyses
San Antonio, TX 78238
USA

Stamatakos
John A.
Center for Nuclear Waste Regulatory Analyses
San Antonio, TX 78238
USA

Ferrill
David A.
Center for Nuclear Waste Regulatory Analyses
San Antonio, TX 78238
USA

Ofoegbu
Goodluck I.
Center for Nuclear Waste Regulatory Analyses
San Antonio, TX 78238
USA

Normal Faulting
Numerical Analysis
Jointed Rock
Joint Aperture
Deformation
Fluid Flow
Radioactive Waste